Research Article

Effects of luffa and glass fibers in polyurethane-based ternary sandwich composites for building materials

J. F. Jamaluddin[1] · A. Firouzi[2] · M. R. Islam[3] · A. N. A. Yahaya[1]

Abstract

Luffa fiber, glass wool (yellow) and glass fiber (white) were used into polyurethane (PU) to prepare sandwich composites. Effects of reinforcement in the composites were evaluated in terms of sound absorbance, water absorption and mechanical properties. In addition, the elastic and plastic nature along with the ignition property of the composites due to the reinforcement of the fibers was also revealed. The thermal properties of the composites were determined by differential scanning calorimetry and thermogravimetric analysis, whereas, the surface morphology of the samples before and after the ignition were examined by scanning electron microscopy (SEM). Result analysis revealed that the PU composites reinforced with glass fiber (white) showed the highest sound absorbance (21.3 dB) and tensile strength (0.96 MPa) compare to the others. The thermal stability was enhanced by 10 °C due to the reinforcement of the glass and luffa fiber. The glass transition temperature was increased significantly (58 °C) by the addition of glass fiber. The sound absorption coefficient changed from 0.21 to 0.27 due to the incorporation of the glass fiber. A large number of different-sized pores created in the composites as observed from the SEM analysis.

Keywords Luffa fiber (LF) · Polyurethane (PU) · Glass fiber (GF) · Composites · Sound insulation

1 Introduction

Natural fibers (NFs) have become promising alternative as a reinforcing agent for polymer composites. Previous works using NFs in polymer composites focused mostly on thermal, mechanical and structural properties. The documented results were impressive. Reports highlights that the uses of NFs have some advantages due to their intrinsic properties, like light-weight, low-density, renewability and environment-friendly nature. NFs are majorly composed of lignin, hemicellulose, cellulose, pectin and waxes [1, 2]. A number of plant fibers, such as banana, coir, kenaf, jute, pineapple, cotton, and *Luffa cylindrica* (luffa fiber) used successfully for the reinforcement purpose in different polymeric matrices [3]. Despite of the

facilities, NFs show some drawbacks, such as their hydrophilic nature, poor compatibility with polymer and high moisture absorption [4]. These drawbacks can be solved using different treatment on the surface of the fibers and by different types of coupling agents [3, 4].

Luffa is commonly known as sponge gourd, vegetable sponge, bath sponge or buah petola (malay), a member of the species of cucurbitaceous family [5]. It has a cylindrical and smooth shape. It is biodegradable and renewable [6]. LF is one of the mostly used NFs which is widely available all around the world [7]. The most important thing of this fiber is its special type of macro-structure. Its strong fibers are arranged like a bundle and linked with a multiple number of branches, like a bird-nest. This special arrangement

✉ M. R. Islam, remanraju@gmail.com; muhammad.remanul@unikl.edu.my | [1]Malaysian Institute of Chemical and Bioengineering Technology, University of Kuala Lumpur, 78000 Bandar Alor Gajah, Melaka, Malaysia. [2]Department of Biomedical Engineering, University of Houston, Texas, USA. [3]Section of Instrumentation and Control Engineering, Malaysian Institute of Industrial Technology, University of Kualalumpur, 817500 Bandar Seri Alam, Pasir Gudang, Johor, Malaysia.

of fibers can hold a number of voids inside and can be used as insulating materials for sound and heat.

Polyurethane foams have been used in a wide variety of applications, such as cushion, furniture and insulation materials. There are many types of polyurethane foam, for example, polyurethane foam caulking, single component foam sealant and two-component foam insulation or sealant kits [8–10]. Polyurethane foams are made up of a solid and gas phase mixed together to form a foam. This process occurs by combining these two phases in a smooth fashion. The resulting foam has a polymer matrix with either air bubbles incorporated in it, which is known as closed-cell or open-cell structure. Closed-cell foams are generally more rigid, while open-cell foams are usually flexible [8]. The microscopic voids, created during polymerization, have made this polymer light-weighted and to be used for acoustic insulation purpose. Recently, the polyurethane industry has been focused on doing research on anti-flammability of PUs. Their high flammability has limited their utilization in different applications [11]. In this research, both the NF and synthetic fibers were used as a reinforcement for sound and fire resistant purpose. A number of studies have been carried out for the acoustic performance of NF-based polymer composites for improved sound absorption [12, 13]. Both the studies investigated the effect of fiber loading and thickness of the samples on sound absorption properties. A summarize analysis for the acoustic performance of the fibrous and bio-based materials has been documented. Both the empirical and micro-structural model have been discussed to predict the noise absorbance performance of these materials [14, 15]. The especial structural and physical properties of both the synthetic and natural fivers like hollow, porous, spongy, light weight, low density, etc. have always been enlighten in favor of high performance or improved acoustic properties [16, 17].

Glass fibers have been used in various industries, such as automobile and marine. They have been used for composite preparation due to their excellent properties like high strength, flexibility and chemical resistivity. There are different types of glass fiber available, for example, chopped strand, yarns, fabrics and mats. They are different in nature and have unique properties [18, 19]. However, some disadvantages have also been noticed for the using of glass fibers, such as high cost, variable performance, poor repair ability and low process ability. In addition, high energy requirement for the production of glass fiber is another challenge [18]. However, they can be used in low amount as a reinforcing agent with PU foam.

The aim of this research was to find the effects of using both the luffa and glass fibers in polyurethane-based hybrid composites for sound and fire insulation have been extensively researched. A comparative analysis was carried out among the composites for their different performance in the terms of sound absorption and fire resistivity. In addition, their thermal stability, water absorption characteristics and mechanical properties were also evaluated. Moreover, the dispersion and arrangement of the fibers inside the composites was also revealed though scanning electron microscope.

2 Methods

2.1 Materials

The luffa fibers were collected from the local farmers at Kuching, Malaysia, although it can be found all everywhere in Malaysia as it is a local common vegetable. The scientific name of the species is *Luffa aegyptiaca*. It has a density of 0.92 g/cm^3. It consists of cellulose (63%), hemicellulose (20.9%), lignin (11.7%) and ash (0.4%). The fiber was used for the fabrication of the composites without any modification. The Bossman General-purpose polyurethane (PU) spray, (CAS no 9009-54-5), was purchased from Kepong, Malaysia. The foam expands and cures by the moisture present in the air. For safely handling, the spray/vapor was avoided to inhale. The spray was used in well-ventilated area to avoid any unwanted accident. The density of PU foam was approximately 0.07–0.11 g/cm^3. It is insoluble in water. It has a pH of 6.4–8.5. The glass fibers (CAS no. 65997-17-3) were supplied from Poly Glass Fibre Insulation, Prai, Malaysia. Two types of glass fibers: long white colour thread glass fiber and needled yellowish colour glass fiber, were used in this research. Both the two types of glass fiber has a density of 2.2–2.69 g/cm^3.

2.2 Preparation of the composites

Different types of PU-based composites were prepared using a cylindrical mold. The composites were prepared with double layers of natural luffa fiber, glass fiber and glass wool. A thin layer of wax was applied on the inner surface of the mold for easy-release of the samples. The luffa fibers were cut to square size (15 cm × 10 cm) mat of thickness 2 mm, whereas glass fibers mat (thickness = 1 mm, area = 150 cm^2) were inserted as it is collected from the rolling. Both the fibers are oriented vertically in layers (fit and adjusted to the cylindrical mold) in the mold and then, the spray of PU foam was applied into the mold. Nearly, 0.5 ml of PU spray was required to prepare 75 cm^3 volume of a cylindrical mold. The one component PU spray was shaken for 40 s before the application. It was associated with a plastic adaptor and a gun for foam application. The ambient temperature was ensured 23 ± 2 °C. The spraying of the PU foam was

conducted almost at similar flow rate. The tack free time was estimated 12–15 min. After that, the mold was kept in open place for couples of hours, until the PU becomes solidified foam. The solid and cured foam was cut after 20 min. Safety precaution was ensured by wearing mask, goggles and gloves to avoid unwanted inhalation and contact of the spray. It was also ensured that the area was completely safe and isolated from any kind of heat, sparks, flames, and electricity. The schematic illustration of the samples are presented in Fig. 1.

3 Experimental

3.1 Fourier transform infrared (FTIR) spectroscopy

A Fourier transform infrared spectrophotometer (model-Thermo SCIENTIFIC, NICOLET AVATAR 370DTGS, USA) was used to examine the functional groups of the samples. ASTM D5477-18 was followed to perform the testing [20]. The KBr method was employed for the analysis with the scanning ranges from 400 to 4000 cm^{-1}.

LF

PU
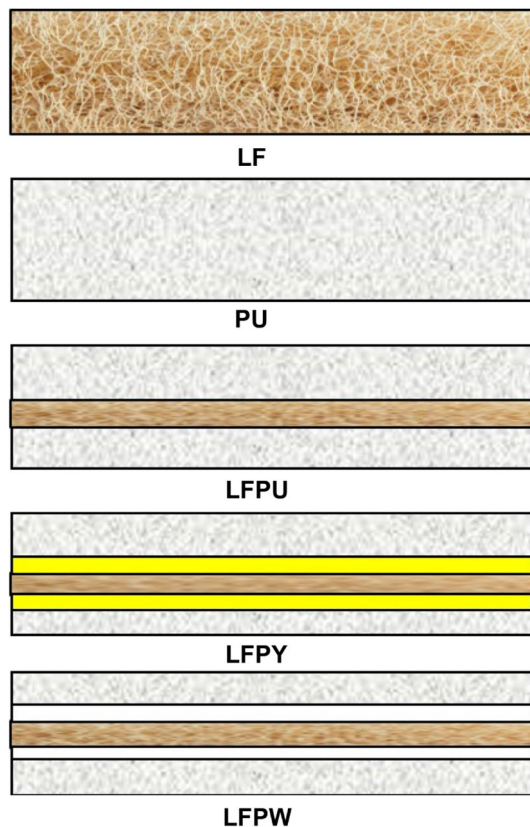
LFPU

LFPY

LFPW

Fig. 1 Schematic illustration of the sandwich composites

3.2 Thermogravimetric analysis

A thermogravimetric analyzer, TA simultaneous instrument (model-TGA/DSC 1), was used to determine the thermal decomposition behavior of the samples. Nearly, 10 mg of the samples was considered for the testing, using a platinum pan. ASTM E2402-19 was adopted to perform the testing [21]. The heating rate was 20 °C/min with the temperature range of 30–600 °C.

3.3 Differential scanning calorimetry

For the melting behavior, a differential scanning calorimeter (Mettler Toledo, TA-GC 10, Model: DSC 822e), was used in a nitrogen atmosphere. ASTM D7426-08 was followed to perform the testing [22]. An aluminum pan was used for the testing with a heating rate of 20 °C/min and the temperature range of 30–400 °C.

3.4 Tensile property

The tensile testing was conducted according to ASTM D638-03 [23]. The sample length, thickness and width was 63.5, 3.16, and 9.8 mm, respectively. The specimens were tested by using a SHIMADZU (model AG-1) universal testing machine (load cell = 1 kN, crosshead speed = 1 mm/min). The test was performed until the tensile failure occurred. Five specimens were tested for each batch and their average value was considered for the analysis.

3.5 Water absorption

The water absorption test was conducted by immersing the specimens in a container, filled with distilled water at 25 °C. ASTM D570-98 was used to perform the testing [24]. After immersion for 1 day, the specimens were taken out from the water and all surface water was removed with a clean tissue paper. The specimens were weighed using an analytical balance. The water absorption was calculated by the weight difference. The percentage of weight gain of the samples was measured by the Eq. 1 [18].

$$WU(\%) = \frac{W_f - W_i}{W_i} \times 100 \qquad (1)$$

where w_i and w_f are the initial and the final weights of the sample before immersing in water and after taking out of water, respectively.
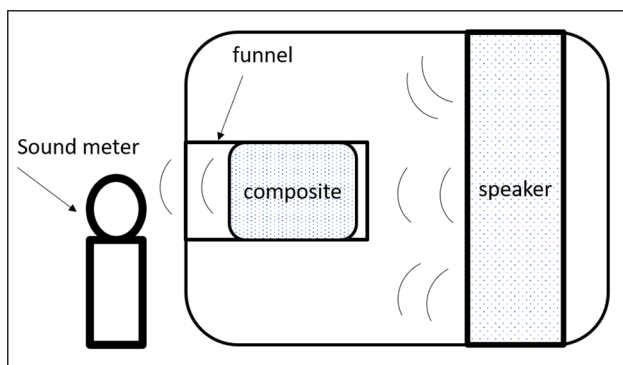
Fig. 2 Schematic illustration of the arrangement of sound absorbance device

3.6 Sound absorption

The sound absorption testing was conducted according to ASTM E1050 [25]. The mechanism for the testing are displayed in Fig. 2. The frequency range was 31.5 Hz to 8.5 kHz. These tests were conducted by placing the samples in the testing chamber as seen in the figure. The sound level of 100 decibel was used as the maximum range. The sound was played without no sample in the chamber to get the blank reading of the sound level. After that, all the samples were placed one after another and sound absorption level was tested. The specimens were placed in a funnel which was also placed in between of the source, speaker, and a digital receiver. The data was displayed in the recorder.

3.7 Ignition test

Finally, the samples were tested for the ignition property analysis. A part of his test was carried out to observe the ignition or burn-characteristics of the composites, following the UL94 test method, qualitative analysis for the flammability of the polymeric materials [26]. The dimension of the bar-shaped test specimen was $15 \times 6.5 \times 3$ cm^3. The testing was performed vertically igniting the samples by burner. This test was conducted by igniting the composites in the direct fire to observe the flammability, amount of smoke produced and how long the fire continues before they become ash.

## 3.8 Scanning electron microscopy

The surface of the fractured (from the tensile testing) as well as the burned samples of the composites was observed by a scanning electron microscope (model-Phenom ProX, The Netherlands). ASTM E1829-14 was followed to perform the observation [27]. The samples were completely dried before testing. Then the samples were mounted onto a metal based holder with the help of double sided sticky carbon tape. Then the coated sample were exposed for microscope imaging at 15 kV.

4 Results and discussion

4.1 FTIR analysis

The FTIR spectroscopic analysis was used for the functional structure of the fibers and the composites. Figure 3 shows the IR spectra of different samples. The spectra for different samples are presented in Table 1. Referring to the FTIR spectra of LF, it was found that the OH stretching of alcohol/hydroxyl group can be confirmed by the peak at around 3343 cm^{-1}. The presence of C–H stretching can be confirmed by the peak at 2958 cm^{-1}. In addition, a number of typical peaks, for example, C=O stretch, C–H stretch, C–O stretching vibration and C–O–C stretch were confirmed by the peak at 1732 cm^{-1}, 1492–1595 cm^{-1}, 1232 cm^{-1} and 1019–1103 cm^{-1}, respectively [28–30]. Refereeing to the FTIR spectra of PU, it was found that the presence of hydroxyl functional group can be confirmed by the peaks at around 3298 cm^{-1}. The presence of C–H stretching was confirmed by the peak around 2917 cm^{-1}, whereas, the evidence of CH$_2$ stretching was noticed by the peak at 2849 cm^{-1}. The isocyanate group was confirmed by the peak at around 2250 cm^{-1}. In addition, the presence of C=O stretching, C–H stretching, CH$_3$ and CH$_2$ symmetrical bending, C–O stretching and C–O–C stretching vibration were noticed by the peak, respectively, at 1726 cm^{-1}, 1509–1537 cm^{-1}, 1434 cm^{-1}, 1229–1307 cm^{-1} and 1072–1148 cm^{-1}.
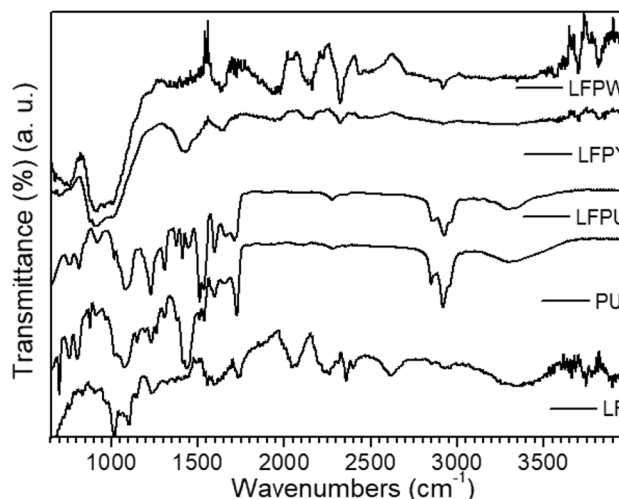
Fig. 3 FTIR spectra of different samples

Table 1 FTIR spectra of different samples

Samples	LF	PU	LFPU	LFPY	LFPW	Assignment
Wavenumbers (cm^{-1})	3343	3298	3297	3346	3347	OH stretching
	2958	2917	2925	2900	2917	C–H stretching
	–	2849	2856	–	–	C–H$_2$ stretching
	–	2250	2276	2322	2322	Isocyanate
	–	–	–	2161	2161	Carbodiimide
	1732	1726	1712	–	1710–1756	C=O stretching of acetyl or carboxylic acid
	1492–1595	1509–1537	1536–1509	1637	1514	Aromatic bending C–H (ring)
	–	1434	1444	1429	–	CH$_3$ and CH$_2$ sym. bending pyran ring
	–	–	1376	–	1382	C–H bending
	1232	1229–1307	–	–	–	C–O stretching
	1019–1103	1072–1148	–	–	–	C–O–C stretching

A comparative analysis of the FTIR spectra of the PU-based composites, such as LFPU (luffa fiber/polyurethane), LFPY (luffa fiber/polyurethane/yellow glass fiber) and LFPW (luffa fiber/polyurethane/ white glass fiber), are presented in Fig. 4. It was found that the presence of hydroxyl groups can be confirmed for all the composites in the area of 3200 to 3400 cm^{-1}. The C–H stretching can be confirmed by the peak at around 2925 cm^{-1}, 2900 cm^{-1} and 2917 cm^{-1}, respectively for LFPU, LFPY and LFPW. The CH$_2$ stretching was found to be shifted to 2856 cm^{-1} due to the incorporation of NFs. The isocyanate group was also found to be evidenced by the peak at around 2276 cm^{-1}, 2322 cm^{-1} and 2322 cm^{-1} for the case of LFPU, LFPY and LFPW. The C=O stretching vibration was shifted to the peak at 1712 cm^{-1} and 1710 cm^{-1} for LFPU and LFPW, respectively. The C–H stretching vibration of the aromatic ring can be confirmed by the presence of peak at around 1509 cm^{-1}, 1376 cm^{-1} and 1514 cm^{-1}, respectively, for LFPU, LFPY and LFPW [28–30]. The CH$_3$ and CH$_2$ symmetrical bending presence was confirmed by the peak at around 1444 cm^{-1} and 1429 cm^{-1}, respectively for LFPU and LFPY. The peak at around 2161 cm^{-1} was confirmed due to the presence of carbodiimide for LFPY and LFPW.

4.2 Thermal stability analysis

The TGA analysis of LF, PU, LFPU, LFPY and LFPW is presented in Fig. 4a. The analysis presents the weight loss (%), thermal stability and percentage of char residue of the samples. The thermal properties of the samples are presented in Table 2. From the figure, it was found that the degradation of LF around 100 °C was due to the loss of moisture, which was also evidenced for LFPU. After that, the NFs experienced degradation for hemicellulose in the period of 200–280 °C, whereas cellulose started degrading from 250 to 350 °C and lignin from 350 to 450 °C. The onset degradation temperature of PU was 243 °C, whereas,

reinforcement with NFs and glass fibers enhanced to 253 °C (LFPU and LFPW) and 253 °C (LFPY). The residues were 28.5, 9.9, 17.8, 23.3 and 22.2%, respectively for LF, PU, LFPU, LFPY and LFPW.

Figure 4b shows the derivative weight vs. temperature curves of the samples. Referring to the graph for LF, it was found that the fiber degraded at three stages: the first stage (T_{max1} = 81.3 °C) was due to the loss of moisture, the second stage (T_{max2} = 255.9 °C) was due to the degradation of cellulose and hemicellulose and finally, the third stage (T_{max3} = 332.9 °C) was due to the decomposition of lignin [31, 32]. On the other hand, PU and composites showed two-stage of degradation. It was found that the rest of the samples degraded at the very first stage (T_{max1} = from 287 to 309 °C), was due to the decomposition of urethane linkages, and the second stage (T_{max2} = from 426 to 437 °C) was due to the degradation of the polyol [31]. The melting behavior of the samples are presented through DSC analysis in Fig. 4c. Regarding the melting behavior of LF, it was found that the curve showed an endothermic start which is probably due to the heat requirement for the removal of moisture [1]. The glass transition temperature (T_g) of PU was 49 °C, which was increased to 91 °C due to the incorporation of LF. On further adding of GF (Y) and GF (W) improved the T_g to 107 °C. This improvement can be attributed as the reinforcement effect of high strength GF. The melting point of PU, LFPU, LFPY and LFPW was in the range of 305–308 °C. The melting behavior of the composites were almost similar for the reinforcement of different fibers.

4.3 Tensile property

The tensile strength (TS) and tensile modulus (TM) of LF, PU, LFPU, LFPY and LFPW are shown in Fig. 5a. The elongation at break (%) of the samples are listed in Table 3. From the figure, it can be seen that the TS and TM of LF was
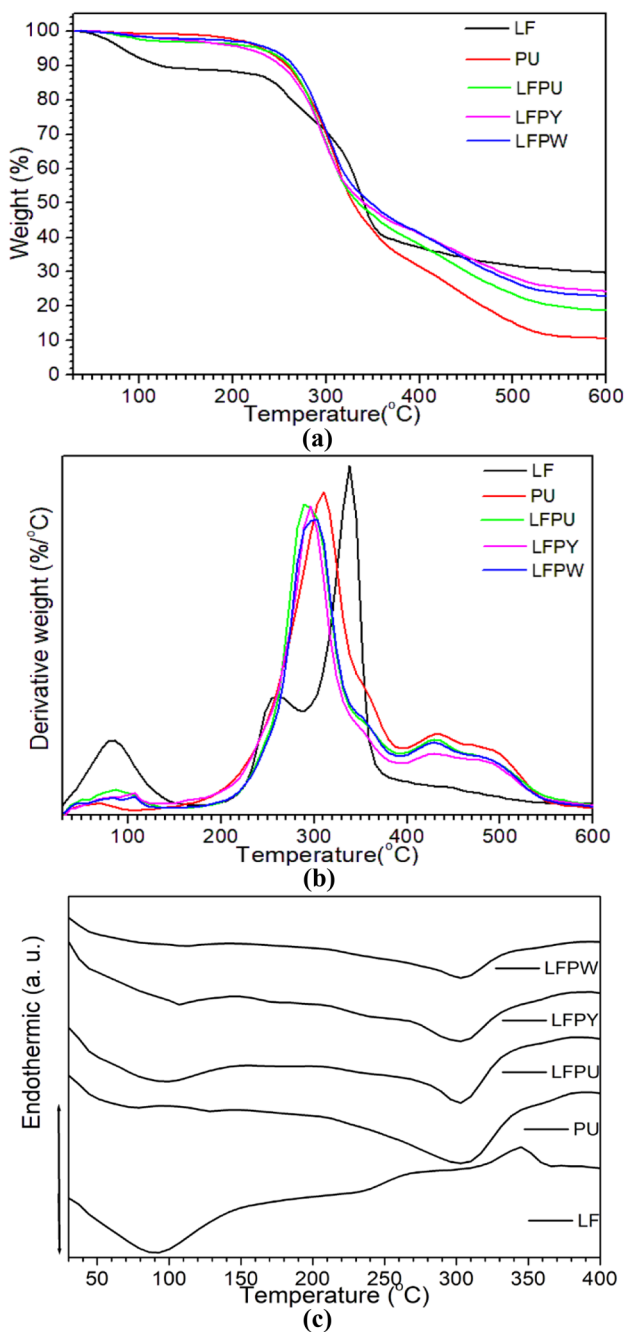
Fig. 4 Weight (%) versus temperature (°C) (**a**), derivative weight versus temperature (**b**) and DSC (**c**) curves of different samples

0.29 MPa and 7.46 MPa, respectively. On the other hand, the TS and TM of PU was 0.16 MPa and 1.9 MPa, respectively. The LF reinforcement increased the TS to 0.17 MPa, which was improved further to 0.21 and 0.96 MPa for the case of LFPY and LFPW. The TM of LFPU was decreased to 0.96 MPa, whereas the same was increased up to 4.7 and 12.7 MPa for the case of LFPY and LFPW. The elongation at break (%) of LF, PU, LFPU, LFPY and LFPW was 11, 20, 32, 18 and 44%, respectively (Table 2).

The stress versus strain curves of the samples are presented in Fig. 5b. From the figure, it can be seen that the PU shows the elasticity nature before it break down, with a linear or flat response of stress in against of strain. The highest stress was experienced by the LF. On the other hand, the reinforcement of natural fiber showed the lowest stress which was experienced by LFPU, showing the elastic nature of the composite. While comparing with LFPY and LFPW, the LFPY showed both the elasticity and the plasticity. Finally, the LFPW showed a slow elastic nature which ultimately sharply collapsed downward beyond the elastic limit, leading to a permanent and irreversible deformation [33, 34].

4.4 Water absorption

The water absorption performances of the samples are presented in Table 3. NFs absorbed more water compared to synthetic fibers and PU. Results analysis showed that the LF, PU, LFPU, LFPY and LFPW absorbed 107, 22, 46, 118 and 102% of water. It is well-known that the NF is hydrophilic whereas, glass fibers are hydrophobic, but results showed that LFPY and LFPW showed the highest water absorption and absorbed water amount was significantly high. This is probably due to the structure of the formulated composites. A huge number of hollow inside can be seen in LFPY and LFPW. The water molecules may be accumulated in the void spaces. Therefore, the highest amount of moisture was absorbed by the composites. It should be noted that there was no compatibilizer used to formulate the composites, therefore, the interface between matrix and fibers were not strongly bonded, which led to higher amount of moisture absorption by the composites (LFPY and LFPW).

Table 2 Elongation at break (%) and thermal properties of the samples

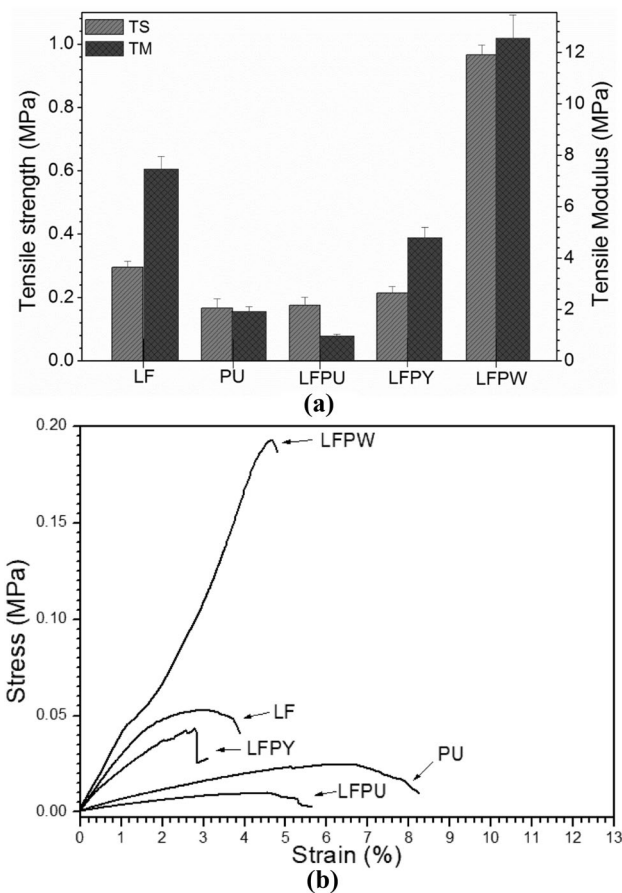| Samples	T_{onset} (°C)	T_{max1} (°C)	T_{max2} (°C)	T_{max3} (°C)	Residue (%)	T_m (°C)	Elongation at break (%)
LF	236	81.3	255.9	332.9	28.5	87.3	11.06
PU	243	297.5	429.1	–	9.9	300.5	20.73
LFPU	253	294.0	435.6	–	17.8	302.6	32.33
LFPY	245	293.9	441.3	–	23.3	302.1	18.94
LFPW	253	297.7	438.9	–	22.2	303.0	44.53

Fig. 5 TS and TM of different samples (**a**) and stress versus strain curves of different samples (**b**)

4.5 Sound absorption

The PU foam and glass wool have been widely used for the sound-proof materials. They have been used in the vehicle exhaust to trap excess sound to avoid any sound or noise pollution. The sound absorption testing was performed to study the presence or influence of fibers in the composites. The sound absorption results are listed in Table 3. Results analysis showed that the LF absorbed least amount of sound at 9.97 dB, while the PU absorbed at 17.63 dB,

nearly twice of sound absorbed by LF. High or compacted airflow resistance always produce a better sound absorption value and give difficulties for sound waves to penetrate to through the materials. The LF showed the lowest sound or noise absorption because the structure of the luffa fiber have lots of holes/hollows that increase the airflows and reduces the sound absorption capability. Then, the surface of perforated PU foam allows the sound waves to enter the interior, inside of the PU foam, thereby decreased the sound reflection [35]. The surface of PU is perforated but it doesn't have much holes like luffa fiber. The sound goes into the PU foam and the reflection was decreased meaning that the sound was being absorbed. On the other hand, the LFPU absorbed noise at 18 dB and the LFPY absorbed noise at 21.3 dB. The most sound or noise absorbed by the LFPY. The LFPW absorbed noise or sound at 20.77 dB. Another factor influences the sound absorption of the materials/composites is the density of the composites. Glass fiber has a density of approximate density 2.2–2.69 g/cm^3 which is the highest among other materials used in this study [36]. The density of LFPU, LFPY and LFPW was 1.52, 1.73 and 1.68 g/cm^3, respectively. The composites having higher density lead to more sound absorption coefficient [37]. In this study, the LFPU. LFPW and LFPY have a high density that can absorb more sound than PU. The reflection of the porosity of density can also affect their sound absorption coefficient value. The sound absorption coefficient of LF, PU, LFPU, LFPY and LFPW was 0.11, 0.21, 0.22, 0.27 and 0.26, respectively. The porous micro-structured materials are preferable for sound absorption in replacement of alternatively used sound insulating materials. In addition, cell size of soft PU foam also contributes in performing sound absorption performance. Regarding this matter, utilizing fibers in PU soft foam can change or reduced down the cell size, as the reduced cell size also responsible for reduced sound absorption coefficient [38].

4.6 Fire ignition analysis

From the ignition testing, different properties like fire-catching, smoke preferences and time of continuation

Table 3 Water absorption, sound absorbance and fire performance of the samples

| Samples	Water absorbed (%)	Sound passed (dB)	Sound absorbed (dB)	Sound absorption coefficient, α	Fire catch	Fire to ash time (s)	Smoke
LF	107.91	90.03	9.97	0.11	Instantly	20	Less
PU	22.05	82.37	17.63	0.21	Instantly	42	More
LFPU	46.52	82	18	0.22	Instantly	50	More
LFPY	118.71	78.7	21.3	0.27	Instantly	102	More
LFPW	102.57	79.23	20.77	0.26	Instantly	95	More

of fire with ash content were determined. The results are tabulated in Table 3. The durability and fire-resistivity were analyzed for all the samples. It was found that all the samples showed the similar nature in terms of fire catching and smoke production, and they catch fire and ignite instantly when the fire source was introduced to the samples. It was noticed that the least smoke was produced from LF. Then, the samples were tested for the time taken for the continuation of the fire. It was found that the LF had the shortest time as 20 s, followed by PU as 42 s, LFPU as 50 s, LFPW as 95 s and LFPY as 102 s. This is because of the fact that the LF had not any barrier that can protect it from direct fire, unlike other samples. For LFPW and LFPY, the maximum time taken for the fire to burn until they turned to the ash. They were affected or manipulated by the presence of glass fiber or glass wool. Fiber glass or glass wool acted as the barrier before the fire could penetrated the composites, which had multiple layers. These multiple layers could be the factor why both composites need more time to turn to ash than other samples. Heat from the fire source needs to penetrate the layers before it can totally ignite

and burn the composites. Furthermore, the glass fiber or glass wool also has high capability to resist the heat to be transferred because of their high heat insulating property. Form the observations, the LF burnt ordinarily like as usual behavior of other dried ligno-cellulosic biomass does. The PU burnt to black ash and melt from the direct fire, whereas, the LFPU burnt from the inside where luffa fiber placed in. On the other hand, LFPY and LFPW burnt finely in shape with some hole appeared and burnt at the part where they were directly exposed on fire. Polyurethane foams produce more smoke than rigid polystyrene, wood, wool and other natural fibers [39]. In addition, the high-density material produced more smoke than low-density material [39]. The amount of smoke production is listed in Table 3. It was found that PU, LFPU, LFPY and LFPW produced more smoke than LF. The fibers acted here as fire-retardant, released higher amount of smoke due to their high density and high value of limiting oxygen index [36, 39]. In addition, the presence of diisocyanate was the main contributor to the smoke and CO [40]. The flammability goes down if the materials show a higher value of limiting oxygen index.

Fig. 6 SEM image of different samples: **a** PU, **b** LFPU, **c** LFPY and **d** LFPW

(a)

(b)
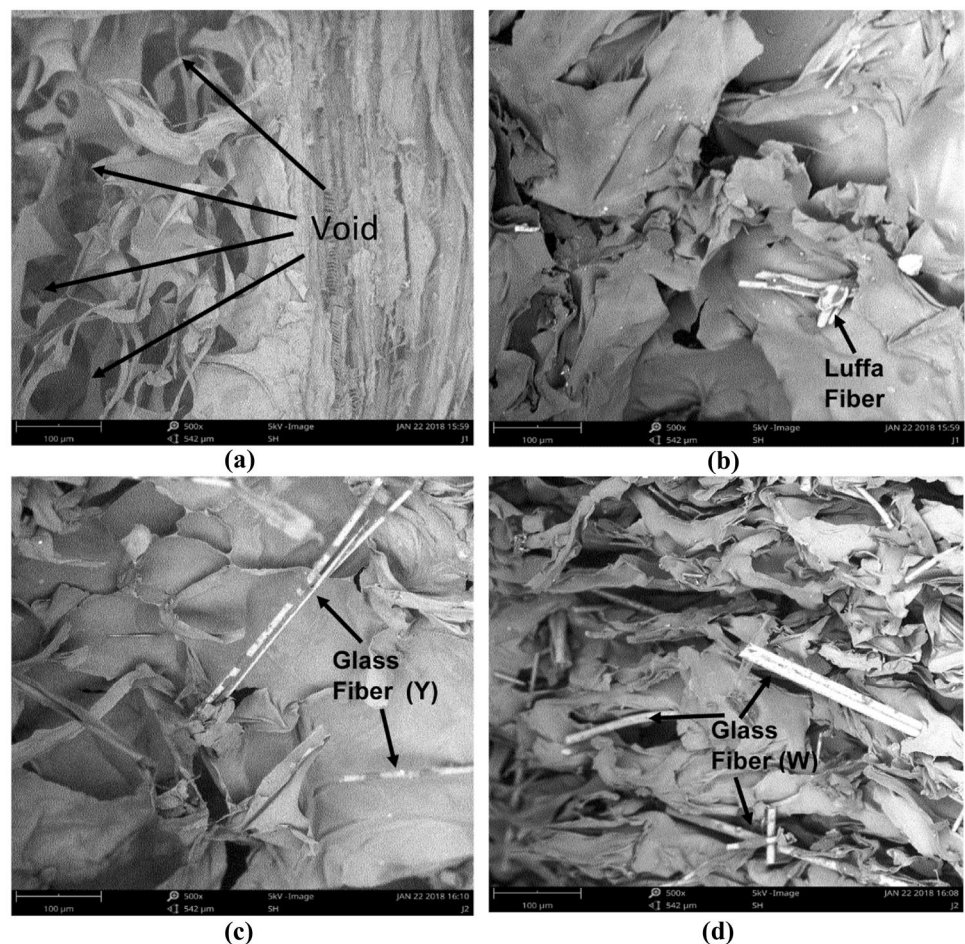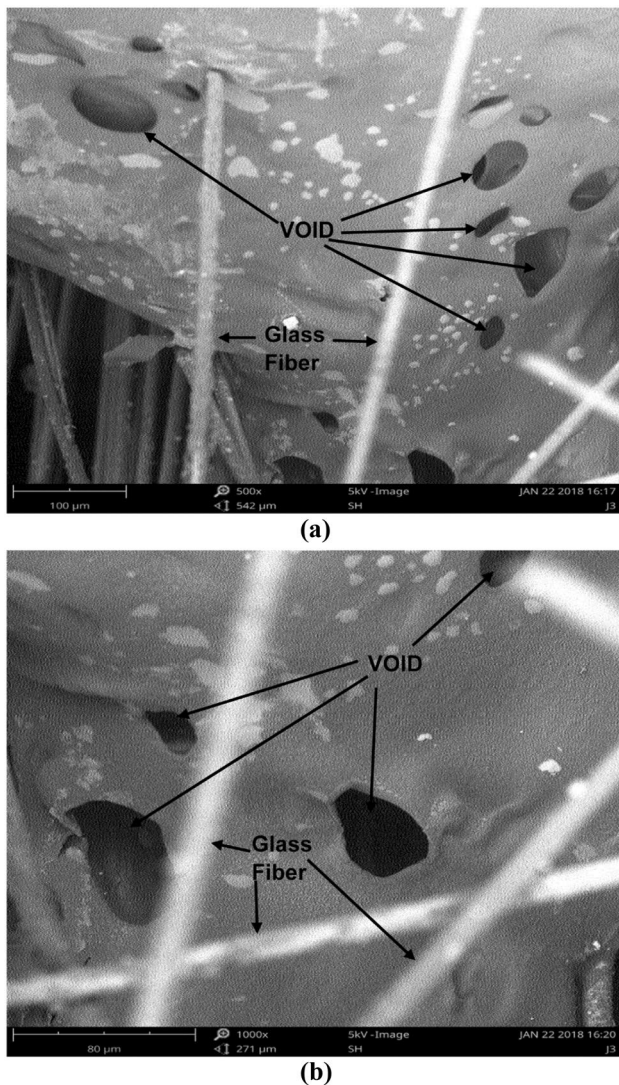
Fig. 7 SEM image of different samples: burned LFPY: **a** low magnification and **b** high magnification

4.7 Surface morphology

The surface of PU, LFPU, LFPY and LFPW are shown in Fig. 6a–d, respectively. It was clearly noticed that the PU foam without fiber shows a number of hollows or voids inside which are dully responsible for low sound absorbance, whereas presence of fiber in it was found to be occupied in the voids, which helped to get better sound absorbance. A relatively less number of voids was observed for the case of LFPU, LFPY and LFPW. Figure 7a, b shows the micrograph of the surface of the composites after the burning process occurred. The samples were considered only for LFPY, with low and high magnification. The long-length of GF was observed with the burned and squeezed surface of PU. The hollow voids and the intumescent pores were formed, indicating the burst-out of the

layers of the polymers formed during the burning process. The pore was created when the non-flammable gases are generated from the materials. Generally, the compactness and protective char layers of them can provide effective thermal barrier to contribute the flame retardant characteristics to the materials [41].

5 Conclusion

A comparative analysis was carried out among the natural fiber and the synthetic fibers (glass fiver and glass wool) for their suitability to be used as reinforcing agents for PU-based foam for heat and sound-proof materials. Result analysis showed that both the glass fibers can be used for heat and sound insulation along with PU foam. The LFPW showed slightly higher melting temperature than other composites. The thermal stability and glass transition temperature of glass fiber based composites increased significantly by 10 °C and 58 °C, respectively. The incorporation of glass fiber also increased the TS and TM by 500 and 668%, respectively. The LFPY and LFPU showed improved performance in terms of sound absorption coefficient (0.27 and 0.26) and fire resistivity. The surface morphology of the composites reinforced with the glass fiber showed more porous structure which helped to improve the sound absorption and ignition properties.

References

1. Sudhir KS, Joyjeet G, Gautam S (2017) Potentiality of luffa fiber used as reinforcement in polymer composites. In: Sapuan S, Alothman O (eds) Jawaid M. Green biocomposites. Green energy and technology. Springer, Cham
2. Alexandre J, Brait V, Manoel J, Henrique L (2016) Effect of fiber treatment condition and coupling agent on the mechanical and thermal properties in highly filled composites of sugarcane bagasse fiber/PP. Mater Res 19(4):746–751
3. Islam MR, Gupta A, Rivai M, Beg MDH (2014) Characterization of ultrasound-treated oil palm empty fruit bunch-glass fibre-recycled polypropylene hybrid composites. J Polym Eng 35(2):1233–1239
4. Islam MR, Isa N, Yahaya AN, Beg MDH, Yunus RM (2017) Mechanical, interfacial, and fracture characteristics of poly (lactic acid) and *Moringa oleifera* fiber composites. Adv Polym Technol. https://doi.org/10.1002/adv.21823
5. Partap S, Kumar A, Sharma NK, Jha KK (2012) *Luffa cylindrica*: an important medicinal plant. J Nat Prod Plant Resour 2(1):127–134

6. Shen J, Min Xie Y, Huang X, Zhou S, Ruan D (2012) Mechanical properties of luffa sponge. J Mech Behav Biomed Mater 15:141–152

7. Kocak D, Merdan N, Yuksek M, Sancak E (2013) Effects of chemical modifications on mechanical properties of *Luffa cylindrica*. Asian J Chem 25(2):637–641

8. Sivertsen K (2007) Polymer foams. 3.063 polymer physics. Springer, Berlin, pp 1–2

9. Akindoyo JO, Beg MDH, Ghazali S, Islam MR, Jeyaratnama N, Yuvaraj AR (2016) Polyurethane types, synthesis and applications – a review. RSC Adv 6:114453–114482

10. Sant'Anna SSE, De Souza DA, De Araujo DM, Carvalho CDF, Yoshida MI (2008) Physico-chemical analysis of flexible polyurethane foams containing commercial calcium carbonate. Mater Res 11(4):433–438

11. Tang Z, Guo B (2017) Flame retardant polymer-halloysite nanocomposites. Functional polymer composites with nanoclays. The Royal Society of Chemistry, London, pp 245–270

12. Ekici B, Kentli A, Kucuk H (2012) Improving sound absorption property of polyurethane foams by adding tea-leaf fibers. Arch Acoust 37(4):515–520

13. Koruk H, Genc G (2015) Investigation of the acoustic properties of bio luffa fiber and composite materials. Mater Lett 157:166–168

14. Tang X, Yan X (2017) Acoustic energy absorption properties of fibrous materials: a review. Compos Part A 101:360–380

15. Zhu X, Kim B-J, Wang Q, Wu Q (2014) Recent advances in the sound insulation properties of bio-based materials. BioResources 9(1):1764–1786

16. Lee HP, Ng BMP, Rammohan AV, Tran LQN (2016) An investigation of the sound absorption properties of flax/epoxy composites compared with glass/epoxy composites. J Nat Fibers 14:71–77

17. Nassar MMA, Arunachalam R, Alzebdeh KI (2017) Machinability of natural fiber reinforced composites: a review. Int J Adv Manuf Technol 88(9–12):2985–3004

18. Islam MR, Rivai M, Gupta A, Beg MDH (2015) Characterization of microwave-treated oil palm empty fruit bunch/glass fibre/polypropylene composites. J Thermoplast Compos Mater 30(7):986–1002

19. Islam MR, Gupta A, Rivai M, Beg MDH, Mina MF (2016) Effects of fibre surface treatment on the properties of hybrid composites prepared from oil palm empty fruit bunch fibres, glass fibres and recycled polypropylene. J Appl Polym Sci 133:43049–43054

20. ASTM D5477-18 (2018) Standard practice for identification of polymer layers or inclusions by Fourier transform infrared microspectroscopy (FT-IR). ASTM International, West Conshohocken

21. ASTM E2402-19 (2019) Standard test method for mass loss, residue, and temperature measurement validation of thermogravimetric analyzers. ASTM International, West Conshohocken

22. ASTM D7426-08 (2013) Standard test method for assignment of the DSC procedure for determining Tg of a polymer or an elastomeric compound. ASTM International, West Conshohocken

23. ASTM D638-03 (2003) Standard test method for tensile properties of plastics. ASTM International, West Conshohocken

24. ASTM D570-98 (2018) Standard test method for water absorption of plastics. ASTM International, West Conshohocken

25. ASTM E1050-19 (2019) Standard test method for impedance and absorption of acoustical materials using a tube, two microphones and a digital frequency analysis system. ASTM International, West Conshohocken

26. The horizontal burning test is used to determine the HB flammability rating of a material. FLAMMABILITY UL 94 HB. https://www.ulttc.com/en/solutions/test-methods/combustion-fire/flammability/ul-94-hb.html. Accessed 1 Jan 2019

27. ASTM E1829-14 (2014) Standard guide for handling specimens prior to surface analysis. ASTM International, West Conshohocken

28. Sathishkumar TP, Naveen J (2014) Glass fiber-reinforced polymer composites—a review. J Reinf Plast Compos 33(13):1258–1275

29. Kaith BS, Chauhan A, Singha AS, Pathania D (2009) Induction of morphological changes. Int J Polym Anal Char 14:246–258

30. Sudhir KS, Joyjeet G, Gautam S, Raghwenda P, Sourabh N (2013) Fabrication, characterization, and evaluation of *Luffa cylindrica* fiber reinforce epoxy composites. BioResources 8(4):4805–4826

31. Yoldas S, Kutlay S, Seckin E, Mehmet S, Gokdeniz N, Cicek O (2010) Characterization of *Luffa cylindrica* fibers and the effect of water aging on the mechanical properties of its composite with polyester. J Appl Polym Sci 123(4):2330–2337

32. Malik SS, Shahzad MK, Tahir J, Waqas A, Muhammad S (2014) Synthesis and characterization of flexible and rigid polyurethane foam. Asian J Appl Sci 2(5):701–710

33. Lewicki JP, Pielichowski K, De La Croix PT, Janowski B, Todd D, Liggat JJ (2010) Thermal degradation studies of polyurethane/POSS nanohybrid elastomers. Polym Degrad Stab 95(6):1099–1105

34. Valcineide OAT, Thais HSF, Sandro CA, Graciela IBM, Satyanarayana KG (2014) Sponge gourd (*Luffa cylindrica*) reinforced polyester composites: preparation and properties. Def Sci J 64(3):273–280

35. Hoda SS (2009) Factors influencing acoustic performance of sound absorptive materials. Aust J Basic Appl Sci 3(4):4610–4617

36. Jia HL, Yu CC, Ting TL, Chen HH, Chien LH, Yueh SC, Ching WL (2016) Effects of perforation on rigid PU foam plates: acoustic and mechanical properties. J Mater 9:1000–1012

37. Anand Nandanwar A, Kiran MC, Varadarajulu KC (2017) Influence of density on sound absorption coefficient of fibre board. Open J Acoust 7:1–9

38. Yamashita T, Suzuki K, Nishino S, Tomota Yo (2008) Relationship between sound absorption property and microscopic structure determined by X-ray computed tomography in urethane foam used as sound absorption material for automobiles. Mater Trans 49(2):345–351

39. Wallenberger FT (2010) Commercial and experimental glass fibers. In: Wallenberger F, Bingham P (eds) Fiberglass and glass technology. Springer, Boston

40. Jaqueline EM (2013) Ignition, combustion and detection of polyurethane foams with ammonium nitrate and sodium bicarbonate additives. Master's thesis, Universidade de Coimbra

41. Liu S-H, Kuan C-F, Kuan H-C, Shen M-Y, Yang J-M, Chiang C-L (2017) Preparation and flame retardance of polyurethane composites containing microencapsulated melamine polyphosphate. Polymers 9:407

Publisher's Note Springer Nature remains neutral with regard to jurisdictional claims in published maps and institutional affiliations.